

Creep behaviour in unloading process of cellulose nitrate under superimposed tensile and hydrostatic loading

T. NISHITANI, Y. DEGUCHI

Department of Applied Mechanics, Suzuka College of Technology, Suzuka 510-02, Japan

The creep behaviour in unloading process under various combinations of superimposed tensile and hydrostatic loading are quantitatively investigated using non-linear-viscoelastic cellulose nitrate heated at 65° C. The creep strain and the creep strain-rate in the unloading process are quite influenced by the effect of hydrostatic pressure, but are not so influenced as those in the loading process mentioned in a previous paper. The deformation properties in the unloading process are also discussed with experiments for proportional loading (namely, uniform rate of stress increases or decreases with time). The stress-strain relation in the unloading process of the creep behaviour under superimposed loading is deduced by using the invariant theory. The deduced relation gives good agreement with the actual observations under the superimposed loading.

1. Introduction

In the previous paper [1], the creep behaviour in the loading process under various combinations of superimposed tensile and hydrostatic loading were quantitatively investigated using non-linear-viscoelastic cellulose nitrate heated at 65° C. The creep strain and the creep strain-rate in the loading process under the superimposed loading were remarkably different from those under uniaxial loading. In the unloading process, the creep behaviour under superimposed loading may be also different from that under the uniaxial loading. Moreover, the creep behaviour in the unloading process is quite different from that seen in the loading process discussed in the previous paper [1].

In the present paper, the creep behaviours in the unloading process under various combinations of superimposed tensile and hydrostatic loading are quantitatively investigated using the same non-linear-viscoelastic cellulose nitrate heated at 65° C as that used to investigate the loading process in a previous paper [1]. In order to find distinctive features of deformation in the unloading process, the deformation behaviour for proportional loading (namely, the uniform rate of stress increases with time in the loading process, or decreases with

time in the unloading process) is also discussed by using the same specimens as used in the creep tests under the superimposed loading. Moreover, as a continuation of the loading process [1], a stress-strain relation of the transient creep in the unloading process is deduced for the non-linear-viscoelastic material subjected to superimposed loading, and the relation is compared with the experimental results. The deduced relation gives good agreement with the actual observations under the superimposed tensile and hydrostatic loading.

2. Stress-strain relationships

2.1. Loading process

By using the time-hardening theory [2] for convenience of analysis, the creep strain-rate for principal strains was proposed as [1]

$$\Delta \dot{\epsilon}_c = B(t+s)^\alpha \Delta \sigma \exp[(b/\sqrt{3}) \Delta \sigma], \quad (1)$$

where t and s denote current time and material constant time, $\Delta \sigma$ is the principal stress difference, and B , α and b are material constants. On the other hand, the instantaneous elastic-plastic strain for principal strains was expressed as [1]

$$\Delta \epsilon_0 = \frac{\Delta \sigma}{2G} \{1 + (\Delta \sigma/\sqrt{3k})^{2n}\}, \quad (2)$$

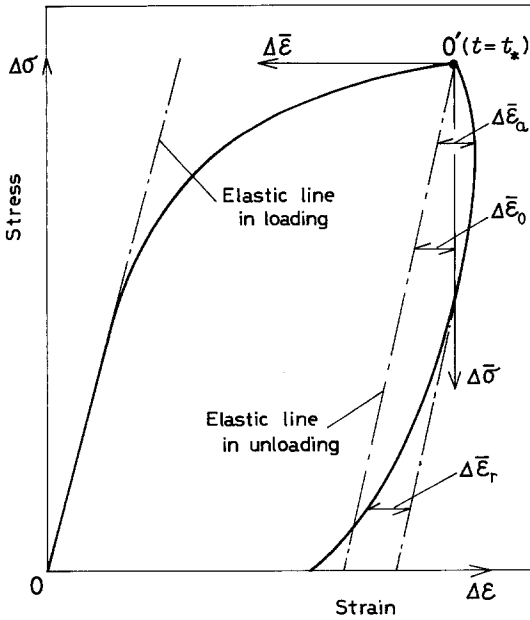


Figure 1 Schematic relation between the stress, $\Delta\sigma$ and $\Delta\bar{\sigma}$, and the strain, $\Delta\epsilon$ and $\Delta\bar{\epsilon}$, for the actual relation, in the loading and unloading processes, respectively.

where G , k and n are material constants. When it is necessary to calculate the total creep strain, $\Delta\epsilon_c$, the following procedure is adopted. Time is subdivided into small intervals, $0 \rightarrow t_1$, $t_1 \rightarrow t_2$, ..., $t_{m-1} \rightarrow t_m$, ..., t , in which the magnitude $\Delta\dot{\epsilon}_c$ may be considered to be approximately constant. For example, $\Delta\epsilon_c(t_m)$ at arbitrary time t_m in the period $t_{m-1} \rightarrow t_m$ is approximated as [1]

$$\Delta\epsilon_c(t_m) = \Delta\epsilon_c(t_{m-1}) + \Delta\dot{\epsilon}_c(t_{m-1})(t_m - t_{m-1}). \quad (3)$$

2.2. Unloading process

The unloading process begins at the last instant $t = t_*$ of the loading process, as shown in Fig. 1, and may be considered as a new loading process beginning at the origin O' of unloading co-ordinate which is corresponding to the instant $t = t_*$. Fig. 1 shows a schematic relation between stress, $\Delta\sigma$, and strain, $\Delta\epsilon$, for the actual relation shown in Fig. 3 which appears later. The axes of the unloading process are directed in opposite directions to those of the preceding loading process. Parameters corresponding to the unloading co-ordinate are distinguished by the addition of a bar superscript to the symbols. Then, at the origin O' of unloading process, $\bar{t} = 0$, $\Delta\bar{\sigma} = 0$, $\Delta\bar{\epsilon}_c = 0$ and $\Delta\bar{\epsilon}_0 = 0$. In the non-linear-viscoelastic deformation of the unload-

ing process, as the instantaneous plastic strain is negligible, the strain, $\Delta\bar{\epsilon}$, in the unloading process is proposed to consist of the three parts, namely, an instantaneous elastic part, $\Delta\bar{\epsilon}_0$, a recovery creep part, $\Delta\bar{\epsilon}_r$, and an additional creep part, $\Delta\bar{\epsilon}_a$, as shown in Fig. 1. As the additional creep strain, $\Delta\bar{\epsilon}_a$, continues to appear in the early stage of unloading process for the operating load, even in the unloading process, this deformation should be also taken into account. The creep strain-rate for principal strains in the unloading process may be expressed by using the same concepts as used in the loading process [1] as

$$\begin{aligned} \Delta\dot{\bar{\epsilon}}_c &= \Delta\dot{\bar{\epsilon}}_r - \Delta\dot{\bar{\epsilon}}_a \\ &= D(\bar{t} + s)^\beta \Delta\bar{\sigma} \exp[(d/\sqrt{3}) \Delta\bar{\sigma}] \\ &\quad - B'(t + s)^\alpha \Delta\sigma \exp[(b/\sqrt{3}) \Delta\sigma], \quad (4) \end{aligned}$$

where the second term on the right-hand side corresponds to the additional creep strain-rate, $\Delta\dot{\bar{\epsilon}}_a$. $\bar{t} = t - t_*$, $\Delta\bar{\sigma} = \Delta\sigma_* - \Delta\sigma$, and $\Delta\sigma_*$ corresponds to the value of $\Delta\sigma$ at time t_* . D , β , d , B' are material constants in the unloading process. However, when the load $\Delta\sigma$ is removed suddenly at the beginning of unloading process, as shown in Fig. 2 (namely, completely unloading creep), the additional creep strain-rate, $\Delta\dot{\bar{\epsilon}}_a$, becomes zero due to $\Delta\sigma = 0$ in the unloading process. Equation 4 may be useful, not only for the creep tests, but for stress rate tests in the unloading process. The elastic strain in the unloading process for principal strains is expressed as

$$\Delta\bar{\epsilon}_0 = \Delta\bar{\sigma}/(2H), \quad (5)$$

where H is material constant. The total creep strain $\Delta\bar{\epsilon}_c$ is calculated by the same procedure as in Equation 3.

3. Experimental procedure

The specimens used were the same as those used in the previous paper [1], and were made of initially isotropic cellulose nitrate of thickness 6 mm. On a surface of each specimen, a square gauge mark was cut in a region of sufficiently uniform stress. The experimental apparatus used was the same as that in the previous paper [1]. The experimental apparatus consisted of three major systems: a high-pressure generator and associated oil vessel with a heater; loading and unloading equipments with a load cell; and instruments to record the load and deformation. Detailed descriptions of the apparatus and of the specimens are given in [3].

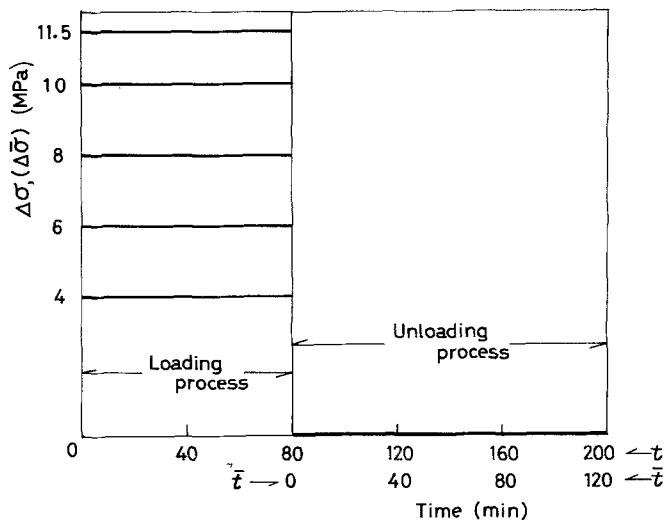


Figure 2 Stress-time diagrams for the loading and unloading processes.

The tests in creep and for proportional loading were performed under superimposed loading of uniaxial tensile stress σ_1 and hydrostatic pressure $\sigma_2 = \sigma_3$ at 65°C , the same as in the previous paper [1]. The combinations of tensile and hydrostatic pressure were adopted as $A = \sigma_{ii}/\Delta\sigma = 1, 0, -1$ and -2 , where A is the dimensionless first invariant of the stress tensor [1], $\sigma_{ii} = \sigma_1 + \sigma_2 + \sigma_3$, and $\Delta\sigma = \sigma_1 - \sigma_2$. The test condition $A = 1$ corresponds to the uniaxial tension ($\sigma_1 = a, \sigma_2 = \sigma_3 = 0$), and $A = -2$ corresponds to the superimposed loading ($\sigma_1 = 0, \sigma_2 = \sigma_3 = -a$). A detailed description of the value A is shown in the previous paper [1].

In order to investigate distinctive features of deformation in the unloading process for polymers, the proportional loading tests in which $\Delta\sigma = \sigma_1 - \sigma_2$ increases linearly with time in the loading process or decreases linearly with time in the unloading process were performed under $A = 1, 0, -1$ and -2 . Each load was applied so as to obtain the constant stress rates of $\Delta\dot{\sigma} = \Delta\dot{\bar{\sigma}} = 1.0$ and 0.1 MPa min^{-1} , where $\Delta\dot{\bar{\sigma}}$ corresponds to the constant stress rate in the unloading process.

The creep tests were performed under $A = 1, 0, -1$ and -2 . The stress-time diagrams for the loading and unloading processes are shown in Fig. 2, that is, each load was applied so as to obtain constant values of $\Delta\sigma = \Delta\bar{\sigma} = 4, 6, 8, 10$ and 11.5 MPa . When the load $\Delta\sigma = a$ is removed suddenly at the beginning of unloading process which corresponds to $t = 80 \text{ min}$ or $\bar{t} = 0$ in Fig. 2, the condition $\Delta\sigma = 0$ corresponds to $\Delta\bar{\sigma} = a$ in the unloading process. In Fig. 2, time $t = 80 \text{ min}$ or $\bar{t} = 0$ corresponds to the last instant of loading

process t_* and corresponds to the original time of unloading process.

Axial elongation and cross contraction between gauge marks engraved on the specimen were measured to within 0.005 mm from photographs of the gauge marks using a magnifying projector. The accuracy of strain thus obtained is within about 2×10^{-4} . The principal strain difference $\Delta\epsilon = \epsilon_1 - \epsilon_2$ was calculated in the natural strain system $e_j = \ln(1 + e_j)$, where e_j ($j = 1, 2$) are the conventional engineering strains.

4. Results and discussions

4.1. Proportional loading tests

Fig. 3 shows the experimental relations between stress $\Delta\sigma$ (or $\Delta\bar{\sigma}$) and total strain $\Delta\epsilon$ ($= \Delta\epsilon_0 + \Delta\epsilon_c$) (or $\Delta\bar{\epsilon}$) in the loading and unloading processes for the proportional loading $\Delta\dot{\sigma} = \Delta\dot{\bar{\sigma}} = 1.0 \text{ MPa min}^{-1}$ at 65°C . Each point is plotted using average values of the three test results. As shown in Fig. 3, in the early stage of the unloading process, the additional creep strain, $\Delta\bar{\epsilon}_a$, stated in Fig. 1 continues to appear, especially for larger values of A . The strains, $\Delta\bar{\epsilon}$, in the unloading as well as, $\Delta\epsilon$, in the loading processes are quite influenced either by the hydrostatic pressure or by the value of A . The effect becomes larger for larger values of A . Moreover, it was found from the present tests and also from the previous tests [4] that the effect of the hydrostatic pressure became larger for smaller values of $\Delta\dot{\sigma} = \Delta\dot{\bar{\sigma}}$.

4.2. Elastic strain in the unloading process of creep tests

Fig. 4 shows the relations between stress $\Delta\bar{\sigma}$ and

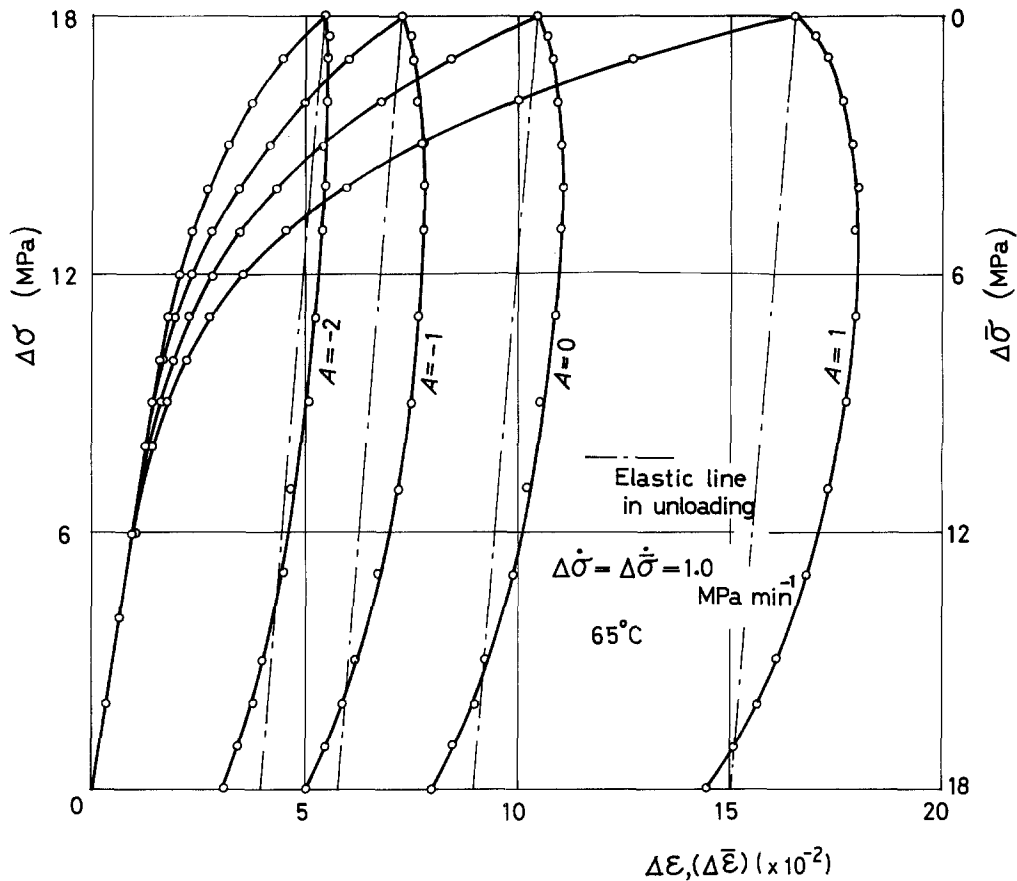


Figure 3 Experimental relations between the stress, $\Delta\sigma$ and $\Delta\bar{\sigma}$, and the strain $\Delta\epsilon$ and $\Delta\bar{\epsilon}$, in the loading and unloading processes for the proportional loading at 65°C .

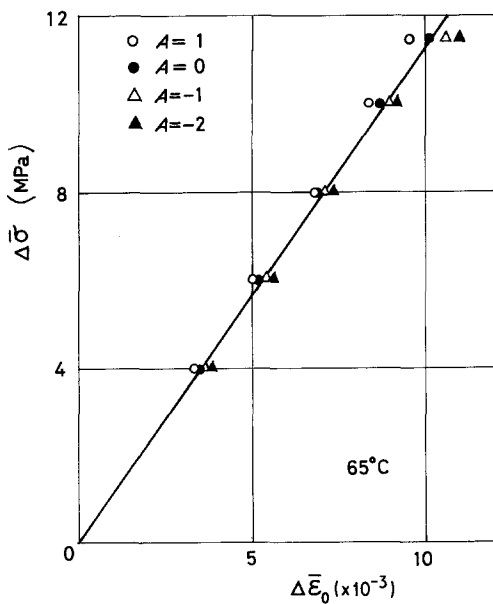


Figure 4 Relationship between the stress, $\Delta\bar{\sigma}$, and the elastic strain, $\Delta\bar{\epsilon}_0$ at the instant of unloading obtained from the creep tests at 65°C .

the instantaneous elastic strain $\Delta\bar{\epsilon}_0$ obtained from the creep experiments at the instant of unloading for each value of A at 65°C . Each point is plotted using an average of three test results. $\Delta\bar{\epsilon}_0$ depends qualitatively on the value of A or on the effect of hydrostatic pressure, and becomes smaller for larger values of A . A proportional dependence in Fig. 4 may be approximately assumed for each value of A . The straight line through the origin of Fig. 4 is drawn using the method of least-square fit, for comparison. The material constant in Equation 5 was determined from the straight line in Fig. 4 as $H = 585\text{ MPa}$.

4.3. Transient creep behaviour in the unloading process

The curves in Fig. 5 show the experimental creep relations between the total strains $\Delta\epsilon$ and $\Delta\bar{\epsilon}$ and times t and \bar{t} in the loading and unloading processes, respectively, for $\Delta\sigma = \Delta\bar{\sigma} = 11.5\text{ MPa}$, as an example, where the loading process corresponds to time interval $t = 0 \rightarrow 80\text{ min}$ and the unloading

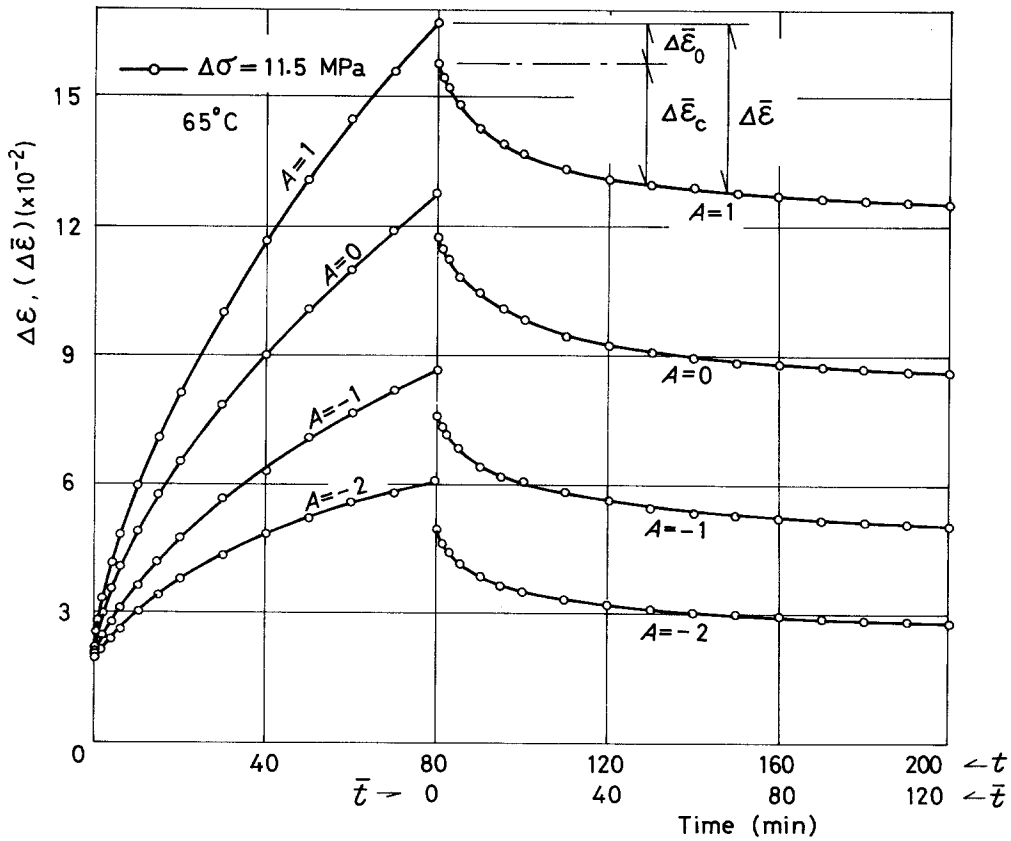


Figure 5 Experimental creep relations between the strain $\Delta\epsilon$ and $\Delta\bar{\epsilon}$ and time, t and \bar{t} , in the loading and unloading processes for $\Delta\sigma = \Delta\bar{\sigma} = 11.5$ MPa at 65°C .

process corresponds to time interval $t = 80 \rightarrow 200$ min. In the region of the unloading process in Fig. 5, the strain $\Delta\bar{\epsilon}$ is divided into the elastic strain, $\Delta\bar{\epsilon}_0$, and the creep strain, $\Delta\bar{\epsilon}_c$. The solid curves in Fig. 6 show the relations between the creep strain-rate, $\Delta\dot{\bar{\epsilon}}_c$, and the unloading time \bar{t} obtained from the corresponding creep curves in Fig. 5. Although the creep strain or the creep strain-rate in the unloading process is quite influenced by the value of A , it is not affected so seriously as in the loading process by the value of A [1].

The value of material constant, B' , in Equation 4 is determined by the following procedure. As the value of H was determined in Section 4.2, the straight line showing $\Delta\bar{\epsilon} = \Delta\bar{\sigma}/(2H)$ can be drawn so as to pass through the original point of unloading process. Each straight line for each value of A is expressed with the thin chain-line in Fig. 3. The distance between the abscissas of the straight line and the unloading curve in the early stage of the unloading process of Fig. 3 may be approximately

considered as the additional creep strain, $\Delta\bar{\epsilon}_a$, corresponding to the second term on the right-hand side of Equation 4. As the values of s , α and b were known in the previous paper [1] as $s = 1.0$ (min), $\alpha = -0.35$, $b = 0.65$ (MPa^{-1}) for $A = 1$, the value of B' is determined as $B' = 9.4 \times 10^{-7}$ ($\text{MPa}^{-1} \text{min}^{-(\alpha+1)}$) for $A = 1$.

The values of the other material constants in Equation 4 are determined from the solid curves in Fig. 6 to be $D = 6.4 \times 10^{-6}$ ($\text{MPa}^{-1} \text{min}^{-(\beta+1)}$), $\beta = -0.66$, $d = 0.58$ (MPa^{-1}) for $A = 1$. The material constants D , d and B' in the unloading process are affected by the value of A or by the effect of hydrostatic pressure, and are shown in the inset to Fig. 6. The dashed curves in Fig. 6 show the relations between $\Delta\dot{\bar{\epsilon}}_c$ and time \bar{t} , calculated from Equation 4 using the corresponding material constants for each value of A . These curves agree well with the corresponding experimental results expressed with the solid curves. The same correspondences were also confirmed for $\Delta\bar{\sigma} = 10, 8, 6$ and 4 MPa.

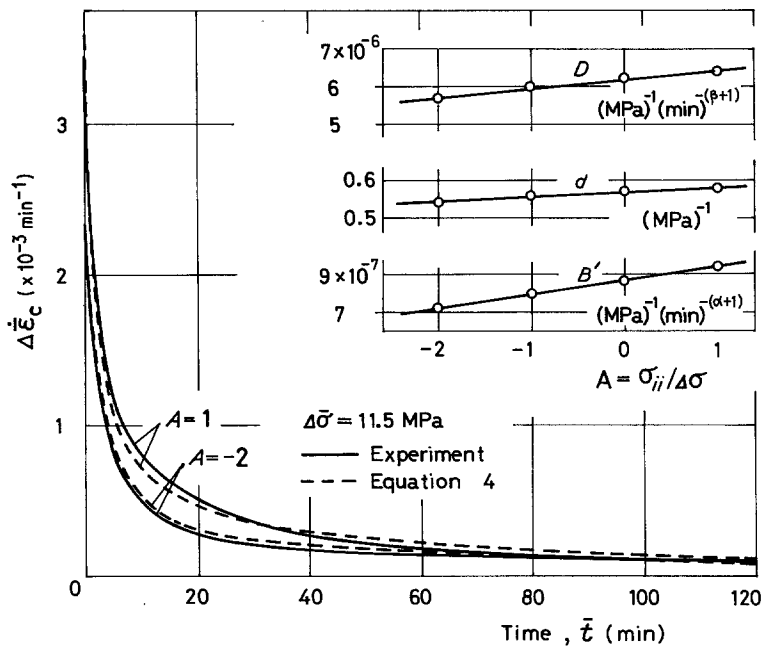


Figure 6 Relations between the creep strain-rate $\Delta\dot{\epsilon}_c$ and time \bar{t} for $\Delta\bar{\sigma} = 11.5$ MPa in the unloading process.

5. Concluding remarks

The main results are

(a) In the unloading process for the proportional loading tests of non-linear-viscoelastic cellulose nitrate, the additional creep strain apparently continues to appear in the early stages of the unloading process due to the operating load, even in the unloading process, especially for larger values of A .

(b) The elastic strain in the unloading process for creep tests of non-linear-viscoelastic cellulose nitrate is qualitatively influenced by the hydrostatic pressure, and have a tendency to increase with increasing the hydrostatic pressure.

(c) The creep strain in the unloading process of non-linear-viscoelastic cellulose nitrate is quite influenced by the hydrostatic pressure, unlike most metals. However, such trend in the unloading process is not so remarkable as that in the loading process.

(d) The proposed stress-strain relation for

creep behaviour of unloading shows good agreement with actual observations of unloading process independent of the values of stress and of the values of A .

(e) These kinds of distinctive features for non-linear-viscoelastic cellulose nitrate mentioned above were also confirmed for non-linear-viscoelastic acetylcellulose in the preliminary tests. It may be considered that the similar phenomena mentioned above may appear in the unloading process for many polymers.

References

1. T. NISHITANI, *J. Mater. Sci.* **12** (1977) 1185.
2. Yu. N. RABOTNOV, "Creep Problems in Structural Member" (North-Holland, Amsterdam, 1969) p. 273.
3. Y. OHASHI, *Brit. J. Appl. Phys.* **16** (1965) 985.
4. T. NISHITANI and Y. MURAYAMA, *J. Mater. Sci.* **15** (1980) 1609.

Received 18 June
and accepted 30 July 1981